

RESEARCH ARTICLE

10.1002/2016WR019994

Key Points:

- Provide and test a Lagrangian scheme to model solute dilution in heterogeneous porous media
- Applies a novel numerical technique to simulate solute spreading and dilution in heterogeneous porous media
- Verify previously proposed expressions to compute grid-scale time-dependent dispersion coefficients for heterogeneous porous media

Supporting Information:

- Supporting Information S1

Correspondence to:

P. A. Herrera,
paulo.herrera.eirl@gmail.com

Citation:

Herrera, P. A., J. M. Cortínez, and A. J. Valocchi (2017), Lagrangian scheme to model subgrid-scale mixing and spreading in heterogeneous porous media, *Water Resour. Res.*, 53, 3302–3318, doi:10.1002/2016WR019994.

Received 28 OCT 2016

Accepted 24 MAR 2017

Accepted article online 1 APR 2017

Published online 21 APR 2017

Lagrangian scheme to model subgrid-scale mixing and spreading in heterogeneous porous media

P. A. Herrera^{1,2} , J. M. Cortínez^{1,3}, and A. J. Valocchi⁴ 

¹Department of Civil Engineering, Universidad de Chile, Santiago, Chile, ²Now at IIDP, Santiago, Chile, ³Now at ARCADIS, Santiago, Chile, ⁴Department of Civil and Environmental Engineering, University of Illinois at Urbana-Champaign, Champaign, Illinois, USA

Abstract Small-scale heterogeneity of permeability controls spreading, dilution, and mixing of solute plumes at large scale. However, conventional numerical simulations of solute transport are unable to resolve scales of heterogeneity below the grid scale. We propose a Lagrangian numerical approach to implement closure models to account for subgrid-scale spreading and mixing in Darcy-scale numerical simulations of solute transport in mildly heterogeneous porous media. The novelty of the proposed approach is that it considers two different dispersion coefficients to account for advective spreading mechanisms and local-scale dispersion. Using results of benchmark numerical simulations, we demonstrate that the proposed approach is able to model subgrid-scale spreading and mixing provided there is a correct choice of block-scale dispersion coefficient. We also demonstrate that for short travel times it is only possible to account for spreading or mixing using a single block-scale dispersion coefficient. Moreover, we show that it is necessary to use time-dependent dispersion coefficients to obtain correct mixing rates. On the contrary, for travel times that are large in comparison to the typical dispersive time scale, it is possible to use a single expression to compute the block-dispersion coefficient, which is equal to the asymptotic limit of the block-scale macrodispersion coefficient proposed by Rubin et al. (1999). Our approach provides a flexible and efficient way to model subgrid-scale mixing in numerical models of large-scale solute transport in heterogeneous aquifers. We expect that these findings will help to better understand the applicability of the advection-dispersion-equation (ADE) to simulate solute transport at the Darcy scale in heterogeneous porous media.

1. Introduction

1.1. Motivation

Solute transport in porous media flow depends upon transport mechanisms that occur at the pore scale. Traditionally, pore-scale processes have been upscaled to obtain equations and effective parameters that describe the dynamics of spatially averaged concentrations defined over the REV (representative elementary volume) scale. At that scale, hereafter referred to as local, continuum, or Darcy scale, solute transport is modeled by an advection-dispersion equation (ADE) that includes the local or hydrodynamic dispersion tensor, \mathbf{D}_L , which includes the effect of molecular diffusion and pore-scale mechanical dispersion, and the local-scale average pore water velocity, \mathbf{v} .

Local-scale dispersion accounts for the interplay between diffusion and spreading caused by pore-scale velocity fluctuations. However, it is widely recognized that many real aquifers display significant heterogeneity in permeability over small scales on the order of centimeters [e.g., Zheng et al., 2011; Dogan et al., 2014]. This heterogeneity leads to fluctuations in Darcy-scale velocity that change the shape of solute bodies, while local-scale dispersion transfers solute mass across zones where concentration gradients exist [Urroz et al., 1995; Weeks and Sposito, 1998]. While spreading creates concentration gradients by increasing the surface of the boundaries of the solute plume, local dispersion destroys them by transferring mass from high to low concentration regions (Figure 1). The net result of the combined action of both mechanisms is to increase the volume occupied by the solute mass and decrease concentration values by mixing waters with high and low solute concentration [Cirpka, 2002; Dentz et al., 2011; de Dreuzy et al., 2012]. Hence, an appropriate description of mixing processes is important for a correct characterization of natural dilution of contaminant plumes and to account for mixing of waters of different composition in reactive transport simulations [Cirpka, 2002; Janssen et al., 2006; Dentz et al., 2011].

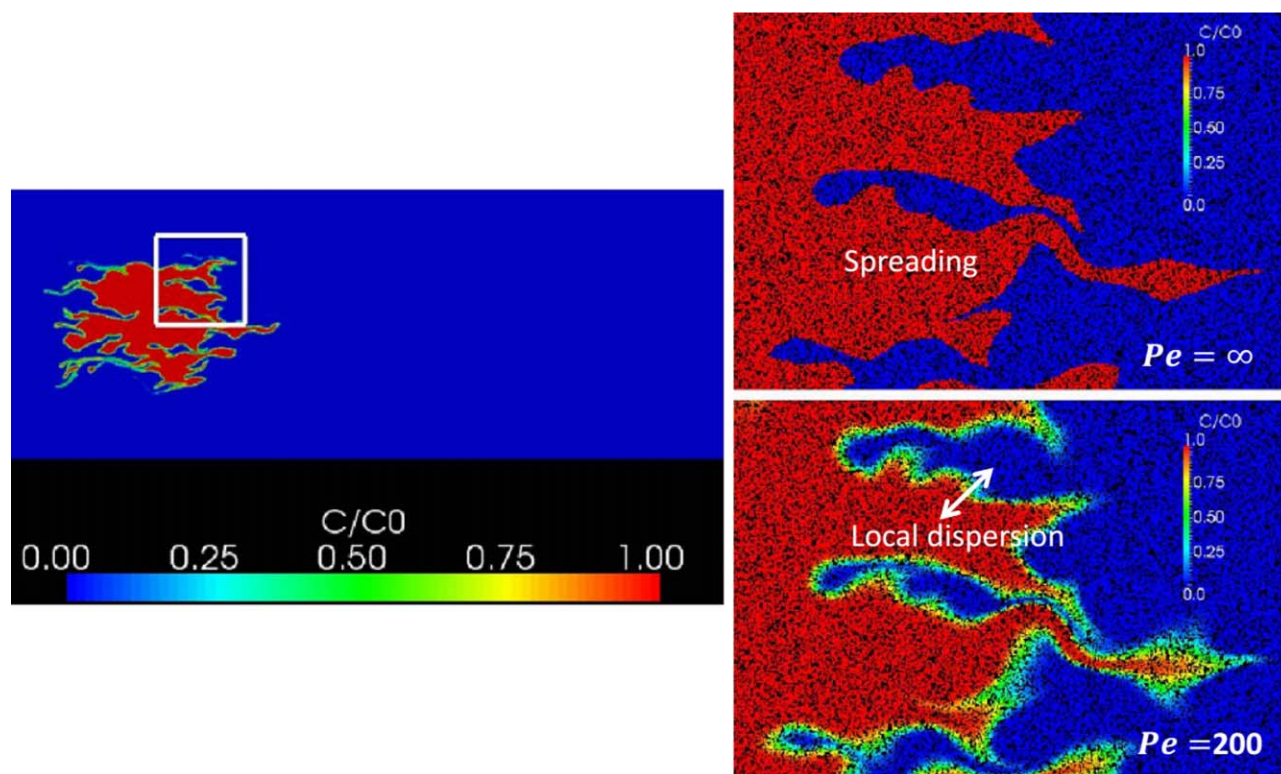


Figure 1. Spreading and mixing in heterogeneous porous media. Fluctuations in Darcy-scale velocity produce changes in the shape of solute plumes, while local-scale dispersion transfers solute mass across zones where concentration gradients exist. Right figures show a magnified view of the white rectangle in the left figure for $Pe = \infty$ and $Pe = 200$.

Application of the local-scale ADE to study solute migration at the regional or aquifer scale presents two main challenges. First, with the exception of very rare situations, it is impossible to collect enough field data to characterize the flow field and transport parameters with enough resolution to apply the local-scale transport model. Second, current computing power available for most applications is limited and unable to simulate regional-scale domains with grid cells small enough to model local-scale concentrations, particularly in reactive transport simulations that consider complex reaction chains that include several chemical components.

To overcome the limited computing power available in most practical applications, it is customary to simulate solute transport using grid cells that are much larger than the local scale, which requires defining new grid-scale transport equations from local-scale equations. The most common grid-scale transport model that is considered in large-scale numerical simulations is an ADE that simulates the evolution of grid-averaged concentrations and includes flow velocities and dispersion coefficients defined at the grid scale. While there are many methods to upscale hydraulic conductivity or flow velocities from fine-scale models [Renard and De Marsily, 1997; De Marsily et al., 2005], there have been many fewer studies that have investigated expressions to calculate grid-scale dispersion coefficients.

Multiple techniques based on a stochastic representation of local-scale parameters have been developed over the last 40 years to compensate for the lack of detailed local-scale data [Dagan, 1989; Gelhar, 1993; Rubin, 2003], and these stochastic approaches have also been used to develop upscaled models at the grid-block scale.

Rubin et al. [1999] (see also follow-up work by Rubin et al. [2003] and Bellin et al. [2004] and work of Eberhard [2005]) derived analytical expressions to calculate grid-scale dispersion coefficients in the presence of mean uniform flow given a local-scale model for the distribution of hydraulic conductivity. The grid-block-scale macrodispersion coefficients were shown to reproduce the rate of spreading of the ensemble-average plume, subject to the underlying assumptions of mildly heterogeneous conductivity and mean uniform

flow. The theory also applies to single realizations under ergodic conditions when the solute plume is much larger than the underlying scale of heterogeneity.

Fernàndez-Garcia and Gómez-Hernández [2007] performed extensive Monte Carlo solute transport simulations in heterogeneous porous media to investigate the impact of upscaling on the evolution of solute plumes. They analyzed the benefits of using block-scale dispersion tensors to compensate for the lack of subgrid-scale information. They found a very good match between block-scale dispersivities calculated numerically and from the theory developed by *Rubin et al.* [1999].

Although the macrodispersion coefficients describe spreading of solute plumes, it is well known that they overestimate mixing. There have been many studies showing that the so-called effective dispersion theory that takes into account finite-size solute plumes more accurately models mixing. Early work on effective dispersion includes *Rajaram and Gelhar* [1993] and *Dentz et al.* [2000a]. A very recent paper by *de Barros and Dentz* [2016] presents complete theoretical results for the mean and variance of block-scale macro and ensemble dispersion coefficients. The results of *Dentz et al.* [2000a] were used by *Cirpka* [2002], who recognized that using the effective dispersion coefficient for a point injection could accurately represent mixing and be used in reactive transport simulations. *Cirpka* also investigated the impact of coarsening the velocity field by sampling the fine-scale $\log(K)$ field on a coarse grid, using kriging to generate a smooth $\log(K)$ field, and solving for flow. By correcting the effective dispersion coefficients to account only for the missing variability, he was able to reproduce the mixing of an ensemble of large plumes, though there was considerable variability among realizations and he was not able to reproduce spreading. Related follow-up work was reported by *Cirpka and Nowak* [2003].

In all the works cited above, block-scale dispersion coefficients included the effect of local-scale dispersion and subgrid velocity fluctuations as a single parameter or through a similar modeling scheme. This makes it impossible to distinguish the respective contribution of subgrid-scale spreading and local-scale dispersion on the simulated mixing rates and dilution processes. Moreover, the use of a single dispersion coefficient implicitly assumes that concentration fluctuations within a grid-block are small so that block-averaged concentrations are good indicators of the mixing processes that occur within each cell. For small times compared to the diffusive time scale, τ_D , and high Péclet numbers which are typical of field conditions [*Dentz et al.*, 2000a, 2000b; *Le Borgne et al.*, 2010; *de Dreuzy et al.*, 2012], spreading caused by velocity fluctuations increases more rapidly than the smoothing effect produced by local dispersion, so that local concentration values can significantly deviate from block-averaged concentration values. This approximation can add significant errors not only in the estimation of mixing rates, but more importantly in reactive transport simulations where the upscaling of reaction rates requires a correct description of higher-order moments of the concentration pdf [e.g., *Chiogna and Bellin*, 2013].

Furthermore, simulations based on traditional grid-based numerical techniques can be affected by large numerical errors that can make it impossible to accurately estimate true mixing rates [*Herrera et al.*, 2009, 2010; *Boso et al.*, 2013]. On the other hand, Darcy-scale RWPT schemes have difficulty to correctly reproduce mass transfer processes due to local-scale dispersion because of the limited number of particles that are used to represent the solute mass distribution. Hence, mixing effects are simulated by averaging particle masses over volumes with finite dimensions [*Salamon et al.*, 2006], which can introduce significant numerical artifacts [*Herrera et al.*, 2009]. Numerical errors due to numerical mixing can be alleviated by using more sophisticated concentration reconstruction techniques [*Fernàndez-Garcia and Sanchez-Vila*, 2011]; however, they cannot be completely removed.

1.2. Objectives

The main objective of this work is to investigate expressions to compute dispersion coefficients that model subgrid-scale velocity information that is not explicitly represented in numerical models. This is important for the typical case when numerical grids have cells that are larger than the typical length scales of the heterogeneity present in natural aquifers. We use a similar hybrid numerical method to the one proposed by *Tartakovsky et al.* [2008] and *Tartakovsky* [2010] to independently evaluate the effect of subgrid-scale spreading and local dispersion on solute mixing. This numerical approach avoids most of the numerical errors that affect other techniques at the expense of increased computational effort. In this work, we present a model that considers Darcy-scale solute transport, where velocity fluctuations are a consequence of fluctuations in hydraulic conductivity. We simulate the effect of subgrid-scale dispersion by adding the

effect of a stochastic velocity component to the displacement of fluid particles, which is modeled based on a time-varying dispersion coefficient. Mass exchange between fluid particles due to dispersion is modeled with a Smoothed Particle Hydrodynamic (SPH) approximation. We extend the analysis to account for the filtering effect of using finite-size numerical grids on the simulated velocity fields. Hence, the main novel contribution of this work is to test expressions to compute block-scale effective dispersion coefficients to simulate spreading and mixing in Darcy-scale solute transport simulations in heterogeneous porous media with a novel numerical Lagrangian framework.

2. Theoretical Framework

2.1. Grid-Averaged Solute Transport Equations

Solute transport in porous media at the local-scale is modeled by the advection-dispersion equation (ADE),

$$\frac{\partial C}{\partial t} + \nabla \cdot (\mathbf{V}C) - \nabla \cdot (\mathbf{D}_L \nabla C) = 0, \tag{1}$$

where C , \mathbf{V} , and \mathbf{D}_L are the local-scale concentration, pore-water velocity, and hydrodynamic dispersion tensor, respectively. It is possible to derive an upscaled transport equation from this equation to use in numerical models, such that the evolution of the cell-block-averaged concentration [Kitanidis, 1988; Dagan, 1989; Gelhar, 1993; Kapoor and Kitanidis, 1997; Rubin, 2003], is described by

$$\frac{\partial \langle C \rangle}{\partial t} + \nabla \cdot (\langle V \rangle \langle C \rangle) - \nabla \cdot (\mathbf{D}_L \nabla \langle C \rangle) + \nabla \cdot \langle vc \rangle = 0, \tag{2}$$

where $\langle \rangle$ denotes spatial average over a grid-block, and lower case letters correspond to zero-mean fluctuations around the mean grid-block value, i.e., $C = \langle C \rangle + c$ and $V = \langle V \rangle + v$. The last expression assumes that there is separation of scales between the subgrid and grid-scale velocity and concentrations such that $\langle VC \rangle \approx \langle V \rangle \langle C \rangle + \langle vc \rangle$ [Beckie, 1998], which is a common assumption made to derive coarse-grained transport equations [e.g., Beckie, 1998; Pope, 2000; Efendiev and Durlofsky, 2003].

The last term in (2) represents the interaction between subgrid-scale velocity and concentration fluctuations [Rubin, 2003]. Since v and c are not explicitly resolved in the numerical grid, this term must be incorporated through a closure model, for example through a Darcy-scale Fickian model such that $\langle vc \rangle = -\mathbf{D}_b \cdot (\langle v(\mathbf{x}) \rangle) \nabla \langle C \rangle$, where \mathbf{D}_b is a block-scale dispersion coefficient. As discussed in the next sections, expressions to estimate that coefficient require a model to describe subgrid-scale heterogeneity in natural formations.

2.2. Heterogeneity Model

Natural heterogeneity present in aquifers involves different spatial scales. For example, it includes large-scale geological features such as geological layers, stratifications, or facies [Scheibe and Freyberg, 1990; Ritz et al., 1994]. The presence of such large-scale units may generate nonstationary flow patterns that are not amenable to traditional geostatistical descriptions [Zhang et al., 2000; Wu et al., 2003; Dai et al., 2004; De Marsily et al., 2005]. Moreover, recent advances in field techniques, such as ground penetrating radar (GPR), used in combination with other field collected data such as results of pumping or slug tests, stratigraphical logs, etc., allow specifying the boundaries of different hydrogeological units [Jadoon et al., 2008; Lambot et al., 2008; Hinnell et al., 2010; Wainwright et al., 2014]. Thus, we can assume that these large-scale features can be deterministically represented in numerical models. Furthermore, the conditioning of numerical models to field data reduces the uncertainty of simulation results [Rubin et al., 1999; Zhang et al., 2000; Cirpka, 2002; De Marsily et al., 2005].

On the other hand, small-scale heterogeneity within each unit is much more difficult to measure and explicitly reproduce in numerical models. It is also reasonable to expect that the magnitude of the fluctuations of properties at this scale are much smaller than at the large scale; thus, they are more amenable to be modeled as stochastic random functions with spatial correlation [Rubin, 2003]. Since our objective is to develop closure models to account only for subgrid-scale heterogeneity, we will consider a traditional correlated Gaussian model to represent the distribution of hydraulic conductivity. We consider that $Y = \log K$ follows a lognormal distribution with expected value m_Y and variance σ_Y^2 . For simplicity, we assume that the covariance of Y is isotropic and exponential with length scale l , i.e.,

$$C_Y(\mathbf{r}) = \sigma_Y^2 \exp\left(-\frac{|\mathbf{r}|}{l}\right). \tag{3}$$

The integral scale, $l_Y = \int_0^\infty C_Y(r) dr$, which measures the spatial persistence of Y , equal to the length scale, i.e., $l_Y = l$ [Rubin, 2003].

2.3. Numerical Algorithm

We propose a numerical approach to simulate solute migration in heterogeneous aquifers that recognizes the multiscale nature of the heterogeneity present in natural porous media and the filtering effect of using a finite size numerical grid. Figure 2 shows why it is necessary to use a fine grid to represent all scales of information contained in a natural flow field. However, most numerical models are based on grids that are only able to represent part of the information contained in the true field. The information of scales smaller than the grid is not explicitly represented on the model. To incorporate the subgrid-scale information, we propose a model that considers that the Darcy-scale velocity of a fluid particle contains two components: a deterministic component at the grid scale and a stochastic one at the subgrid scale, as shown in Figure 3. Mass transfer between neighboring fluid particles due to local-scale dispersion is approximated with a smoothed particle hydrodynamics (SPH) approximation [Tartakovsky et al., 2008; Herrera et al., 2009; Tartakovsky et al., 2015].

To model the stochastic component of the fluid particles velocity, we use a random-walk particle method (RWPT). The magnitude of the random particle displacement is given by a block-scale dispersion coefficient, \mathbf{D}_b , whose estimation is discussed in the next section. The numerical implementation of the RWPT algorithm is based on the axisymmetric formulation of the dispersion tensor proposed by Lichtner et al. [2002]. The components of the dispersion tensor are evaluated using a tri-linear interpolation of the grid-scale velocity to obtain continuity on the dispersion tensor [Salamon et al., 2006].

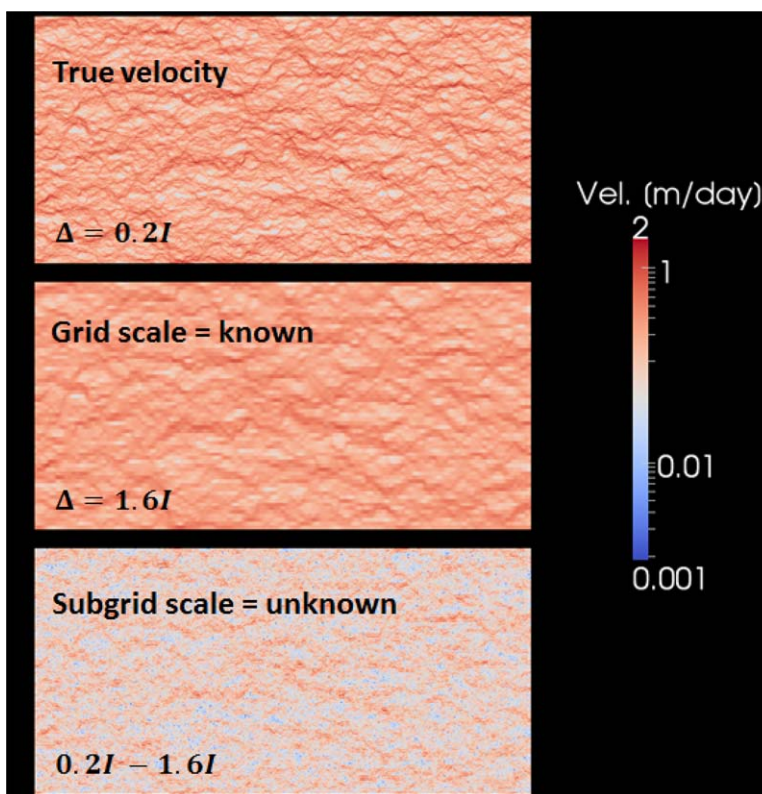


Figure 2. An heterogeneous velocity field (top) represented on a coarse grid (middle) does not contain all small-scale or high-frequency information (bottom), which is filtered by the grid. Colors represent the magnitude of the flow velocity. Thus, the effect of the removed fine-scale information must be incorporated through a closure model, e.g., an effective dispersion coefficient.

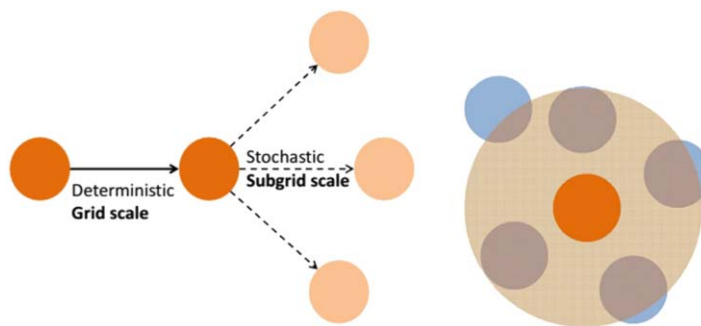


Figure 3. Schematic of the proposed numerical approach to simulate solute migration in heterogeneous aquifers. The movement of a fluid particle contains two components: a deterministic one that is explicitly solved in the numerical model and a stochastic one that accounts for subgrid-scale fluctuations.

ing in an ensemble average sense, i.e., it represents the spreading of a set of plumes that move through aquifers that have the same statistics instead of representing the spreading of an individual plume that moves in a single aquifer.

For plumes that are large enough with respect to the scale of the heterogeneity, D_m becomes ergodic and the ensemble value represents the spreading that takes place in a single realization [Dentz et al., 2000a, 2000b]. For small heterogeneity, i.e., $\sigma_Y^2 \leq 1$, linear stochastic theory allows computation of analytical expressions to calculate D_m [Gelhar and Axness, 1983; Dagan, 1984]. Expressions to compute D_m take into account all scales of heterogeneity present in the aquifer, but are only valid for mild heterogeneity since they are derived based on first-order approximations. D_m depends upon time but it reaches an asymptotic value after the solute plume has traveled on the order of 10 advective time scales $\tau_u = l_Y/U$, where U is the mean flow velocity [Fiori, 1996]. These expressions have been investigated and validated through numerical simulations by several authors [e.g., Bellin et al., 1992; Quinodoz and Valocchi, 1993; Chin, 1997; Salandin and Fiorotto, 1998; Trefry et al., 2003].

Fiori [1996] demonstrated that in general, and in particular for isotropic formations, the effect of local-scale dispersion on D_m is negligible for typical values of Péclet numbers, Pe , found in field situations ($Pe \approx 100-1000$). Thus, it is common practice to neglect the effect of local-scale dispersion in the computation of D_m .

2.4.2. Effective Dispersion

The effective dispersion coefficient, D_e , estimates the rate of growth of the ensemble second central spatial moment calculated for individual plumes. Since D_e is computed from the moments of individual plumes, it is a better estimator for the dispersion that occurs in a single realization than the macrodispersion coefficient [Dentz et al., 2000a, 2000b; Cirpka, 2002].

An important difference with respect to D_m is that, in addition to the initial plume size, D_e strongly depends upon local dispersion [Kitanidis, 1988; Dagan, 1990, 1991]. For the case of a point-like injection with $Pe = \infty$, D_e remains zero for all times since the initial solute plume travels along the streamline that passes through the initial position and does not sample the rest of the heterogeneity of the aquifer. In the presence of local-scale dispersion, D_e is initially equal to local dispersion, D_L , grows with time, and for times larger than $\tau_D = l_Y^2/D_L$, it finally reaches an asymptotic value equal to the macrodispersion coefficient, D_m [Dentz et al., 2000a].

Dentz et al. [2000b] extended the analysis of the effective dispersion coefficient for a large extended initial source. They found that for this initial configuration, D_e reaches its asymptotic limit more rapidly for larger injection regions. They found that for time $\tau_u \leq t \leq \tau_D = \sqrt{(L^2 + l_Y^2)}/D_L$, where L is the length of the initial source transverse to the mean flow, the effective dispersion coefficient is identical to the one for a point-like injection. For typical field values of local-scale dispersion, the effective dispersion coefficient for an initial line source transverse to the mean flow reaches its asymptotic values after the plume has traveled 100–1000 integral scales of the aquifer heterogeneity.

Cirpka [2002] applied the concept of the effective dispersion coefficient in reactive transport simulations. He demonstrated that the application of an effective dispersion coefficient computed assuming a point-like

2.4. Dispersion Coefficients

We next discuss some expressions that have been proposed in the literature to compute dispersion coefficients to model the effect of fluctuations of the Darcy-scale velocity, given a model for the spatial-distribution of the hydraulic conductivity.

2.4.1. Macrodispersion

The so-called macrodispersion coefficient, D_m , models the spreading or increase of the extent of a solute plume with time [Dentz et al., 2011]. D_m quantifies spread-

injection in interpolated coarse-scale fields reproduces the mixing that occurs in fully resolved simulations. However, this was only valid in the ensemble sense because the plumes used were too narrow. In this situation, solute bodies spread differently depending upon their initial position. However, for plumes that are large enough in the direction perpendicular to the flow, such that the ergodicity condition is satisfied, ensemble-averaged quantities can be replaced by cross-sectional averages [Dentz *et al.*, 2000b; Cirpka, 2002]. Then, Cirpka [2002] hypothesized that for larger solute plumes, it could be possible to reproduce the subgrid-scale mixing for single realizations, since D_e for large plumes ($L \rightarrow \infty$) is equivalent to the ensemble average of point-like sources [Dentz *et al.*, 2000b].

2.4.3. Block-Scale Dispersion Coefficients

The macro and effective dispersion coefficients, D_m and D_e , include all the scales of heterogeneity of the aquifer, which makes them unsuitable to be used in numerical models where low-frequency information is explicitly captured in the numerical grid, so that only lost subgrid-scale information must be accounted for through dispersion coefficients [Rubin *et al.*, 1999; Cirpka, 2002; Fernández-García and Gómez-Hernández, 2007]. As noted above, Rubin *et al.* [1999] proposed a block-effective macrodispersion coefficient, D_m^b , and developed expressions to compute it given a geostatistical description of the aquifer heterogeneity under the assumption of mean uniform flow and small σ_Y .

Rubin *et al.* [1999] developed expressions to compute the components of D_m^b , which they demonstrated to be nonstationary but with negligible fluctuations for small variances of $\log(K)$. In general, D_m^b must be characterized by at least its two first moments; however, for large solute plumes that are ergodic with respect to the aquifer heterogeneity and numerical grids with large cells, its variance is small and it can be represented only by its expected value [De Barros and Rubin, 2011]. When the solute plume is larger than about 1.5 times the grid cell size, Δ , the plume can be considered ergodic with respect to the subgrid-scale heterogeneity, and the block-scale macrodispersion coefficient is a good model of the effects of the wiped out variability on solute migration [Rubin *et al.*, 2003]. Some studies have found that the longitudinal component of D_m^b does not depend upon local dispersion for $Pe \geq 100$. For lower Pe , local dispersion reduces D_m^b , particularly for small grid cells [Rubin *et al.*, 1999; Bellin *et al.*, 2004]. An important feature of the block-scale macrodispersion coefficient is that it reaches its asymptotic limit, which is equal to $U l_Y \sigma_Y^2$, where l_Y is the integral scale of the removed subgrid-scale heterogeneity, much faster than D_m after traveling only a few advective time scales τ_u , and thus it can be considered constant in time and space for most practical applications [Rubin *et al.*, 2003].

In order to apply the hybrid numerical approach described above to model the lost subgrid-scale velocity information, we compute a block-scale effective dispersion coefficient that allows us to estimate the movement of fluid particles due to the lost information of the velocity field. We apply expressions proposed in previous works [Rubin *et al.*, 1999; Dentz *et al.*, 2000a; Cirpka, 2002] to compute the block-scale component of D_m^b for spreading and D_e^b for mixing parallel to the mean flow velocity U . Details are given in Supporting Information. Those block-scale expressions are based on applying a high-pass filter to the correlation spectrum of the hydraulic conductivity to remove the information that is explicitly represented in the numerical model, before evaluating the standard expressions for the effective and macrodispersion coefficients.

Figure 4 compares the temporal evolution of D_m and D_e for different values of Pe and grid sizes. While D_m^b reaches its asymptotic value after the solute has traveled only tens of integral scales of the heterogeneity, D_e^b takes much longer time, particularly for advection-dominated transport, i.e., high Pe , as would apply in most field situations. On the other hand, D_e^b reaches its asymptotic limit earlier for lower Pe because larger values of local dispersion will more quickly smooth concentration fluctuations produced by spreading. Similarly, D_e^b reaches its limit more rapidly for smaller grid sizes since the length scale of the subgrid-scale heterogeneity is smaller, hence a solute plume would take less time to sample it.

3. Numerical Simulations

3.1. Simulations Setup

We first generate 2-D spatially correlated $\log(K)$ fields using a spectral method [Robin *et al.*, 1993]. Then, we generate fine-scale flow fields by solving the saturated groundwater flow equation assuming a mean constant hydraulic gradient and no-flow boundary conditions at the top and bottom of the domain. Flow fields are evaluated by a standard cell-centered finite volume approximation. The linear system of equations is

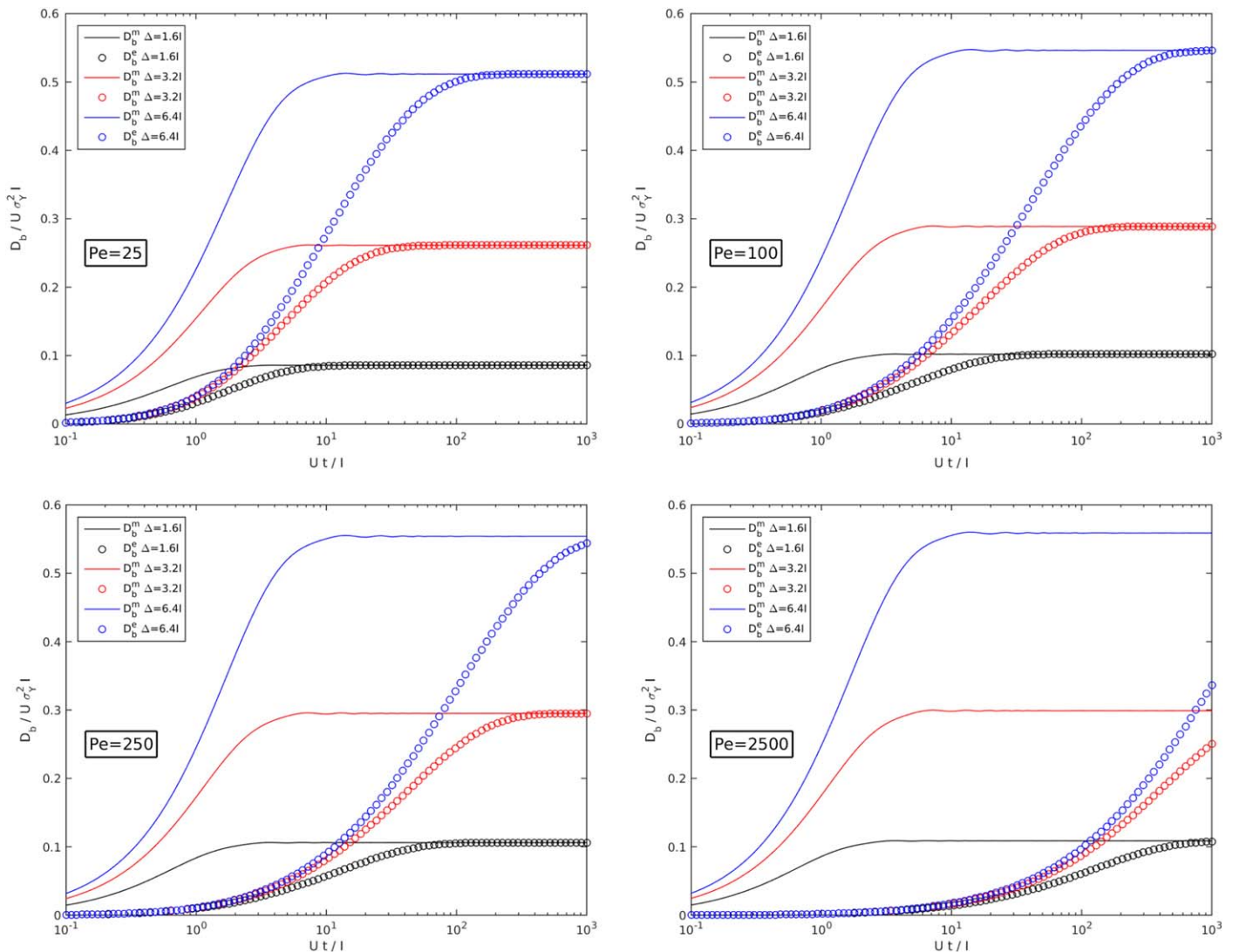


Figure 4. Comparison of block-scale macrodispersion D_b^m (solid lines) and block-scale effective dispersion coefficient for a point-like source D_b^e (circles) for different Péclet numbers (Pe) and grid sizes (Δ).

solved by a preconditioned iterative solver. The tolerance of the iterative solver was set in order to minimize errors in the computation of the flow field that can introduce mass balance issues. The cell size in the fine grid, Δ , was set equal to $0.2l_y$ in order to completely capture the high-frequency information contained in the $\log(K)$ field [Ababou et al., 1989; Chin, 1997; Rubin, 2003]. We used the fine-scale velocity field as a surrogate model of a true groundwater flow field.

Next, we upscale the fine-scale velocity field to generate coarse-scale flow fields. The upscaling procedure consists in applying a sharp filter to the fine-scale flow field in order to remove the high-frequency information. According to the Nyquist theorem, the resulting coarse-scale flow field has only low-frequency information with wave numbers larger than $2\Delta_c$, where Δ_c is the size of the coarse-grid cells [Beckie et al., 1994; Rubin, 2003]. We consider $\Delta_c=16\Delta$ and $\Delta_c=32\Delta$, i.e., coarse cells have areas that are 256 and 1024 times larger than fine cells. The upscaling procedure is mass conservative in the sense that flow rates over the boundaries of the coarse cells are equal to the integral of the fluxes over the fine cells contained on the coarse block.

Solute transport simulations were performed with the hybrid Lagrangian numerical method described above. Grid-scale effective and macrodispersion coefficients were included in the simulations through a random-walk particle tracking algorithm with time-dependent dispersivities to account for the time

Table 1. Parameters Used in Numerical Simulations

Parameter	Value	Description
σ_K^2	1	$\log(K)$ variance
$Lx = Ly$	$204.8 \cdot l_Y$	Domain size
λ_x	$16 \cdot l_Y$	Plume length parallel to mean flow
λ_y	$90 \cdot l_Y$	Plume length transverse to mean flow
Δ	$0.2 \cdot l_Y$	Fine-grid size
Δ_c	$16\Delta, 32\Delta$	Coarse-grid size
$Pe = U \cdot l_Y / D_L$	25, 100, 250, 2500	Péclet number (τ_D / τ_u)
Np	968, 000–1, 317, 600	Number of particles
h	Δ	Smoothing length for SPH approximation

dependency of D_m^b and D_e^b . The effect of local-scale dispersion was simulated with a smoothed particle hydrodynamics (SPH) approximation [Herrera et al., 2009; Herrera and Beckie, 2013], assuming a constant and isotropic dispersion coefficient, i.e., $D_L = D_L$.

The initial plume is a rectangular-shaped region with concentration C_0 and size $16l_Y$ and $90l_Y$ in the

parallel and transverse directions to the mean flow, respectively. These dimensions were chosen in order to simulate a large plume that satisfies the ergodicity condition, such that the effective dispersion coefficient is equivalent to the ensemble dispersion coefficient. At the beginning of the simulation, the initial plume was surrounded by a buffer region with particles with zero concentration to allow for dilution. Since the size of the mixing zone created in each simulation depends upon the value of Pe , the number of particles used in each simulation was dependent on this parameter with a maximum number of more than 1.3 million particles for the simulations with $Pe = 25$. Preliminary tests demonstrated that results did not change if a larger number of particles was used. Table 1 has a summary of the parameters used in the simulations.

3.2. Parameters to Measure Spreading and Mixing

To characterize solute migration, we use parameters to measure spreading and mixing. Traditionally, spreading of the solute plume has been studied by looking at the temporal evolution of the second central spatial moment S_{xx} of the plume position [Rubin, 2003]. Hence, for a set of N_p particles with position $\mathbf{X} = (x, y)$, we compute

$$S_{xx} = \frac{1}{N_p} \sum_{i=1}^{N_p} (x_i - \bar{x})^2, \tag{4}$$

where \bar{x} corresponds to the average position of the particles.

The characterization of mixing requires measurement of changes in the volume of the aquifer that is occupied by the solute plume. Kitaniadis [1994] derived from information theory the concept of dilution index, E , which has been applied in several studies to characterize solute mixing and dilution [e.g., Ursino et al., 2001; Rolle et al., 2009; Chiogna et al., 2012; Boso et al., 2013]. The dilution index is calculated as,

$$E = \exp \left[- \int_V p \ln p \, dV \right], \tag{5}$$

where $p = C(\mathbf{X}, t) / M$ and M is the total solute mass. The integral of the last equation can be numerically approximated considering that the total mass M is distributed among particles that carry individual concentrations. In the presence of local-scale dispersion that distributes the solute mass over larger regions of the aquifer, E grows with time and in a bounded domain with volume V it will eventually reach its maximum value, $E_{\max} = M / V$.

The scalar dissipation rate (SDR) has also been used to quantify mixing in turbulent and porous media flow [Pope, 2000; Le Borgne et al., 2010; de Dreuzy et al., 2012]. It is defined as,

$$SDR(t) = \int_{\Omega} D_L \nabla C(\mathbf{x}, t) \cdot \nabla C(\mathbf{x}, t) \, d\Omega. \tag{6}$$

If solute transport can be modeled by an advection-dispersion equation and there are no mass fluxes through the boundaries of the domain,

$$SDR(t) = - \frac{1}{2} \frac{d}{dt} [SD(t)] = - \frac{1}{2} \frac{d}{dt} \int_{\Omega} C^2(\mathbf{x}, t) \, d\Omega, \tag{7}$$

where $SD(t)$ is known as the scalar dissipation [Pope, 2000]. Since (6) involves computing concentration gradients, it is difficult to evaluate numerically. Thus, it is more convenient to use (7) and evaluate the integral

to compute SD . When (7) is valid, it is possible to demonstrate that $SD(t)$ scales similarly to the concentration variance σ_c^2 , which has also been used in several studies to characterize mixing and dilution in porous media [e.g., Kapoor and Kitanidis, 1998]. For times that are much larger than the dispersive time τ_D , such that the solute plume becomes more similar to a Gaussian plume, SD scales with $t^{-d/2}$, where d is the dimensionality of the problem [Le Borgne et al., 2010; de Dreuzy et al., 2012].

To characterize mixing from the numerical results presented in the next section, we use both parameters: dilution index and scalar dissipation.

3.3. Simulation Results

3.3.1. Spreading

We first compare second central spatial moments for simulations that do not consider local-scale dispersion. Preliminary simulations, not shown here, indicated that even though the initial plume is large enough to satisfy ergodicity, there are large differences in the temporal evolution of S_{xx} for different realizations, which has also been observed in other studies [e.g., Trefry et al., 2003]. Then, to compare solutions for the fine and coarse grids, we take the average of 10 realizations as shown in Figure 5. This number of realizations was chosen because, as also found in previous studies [e.g., Rubin et al., 1999; Trefry et al., 2003], the ensemble

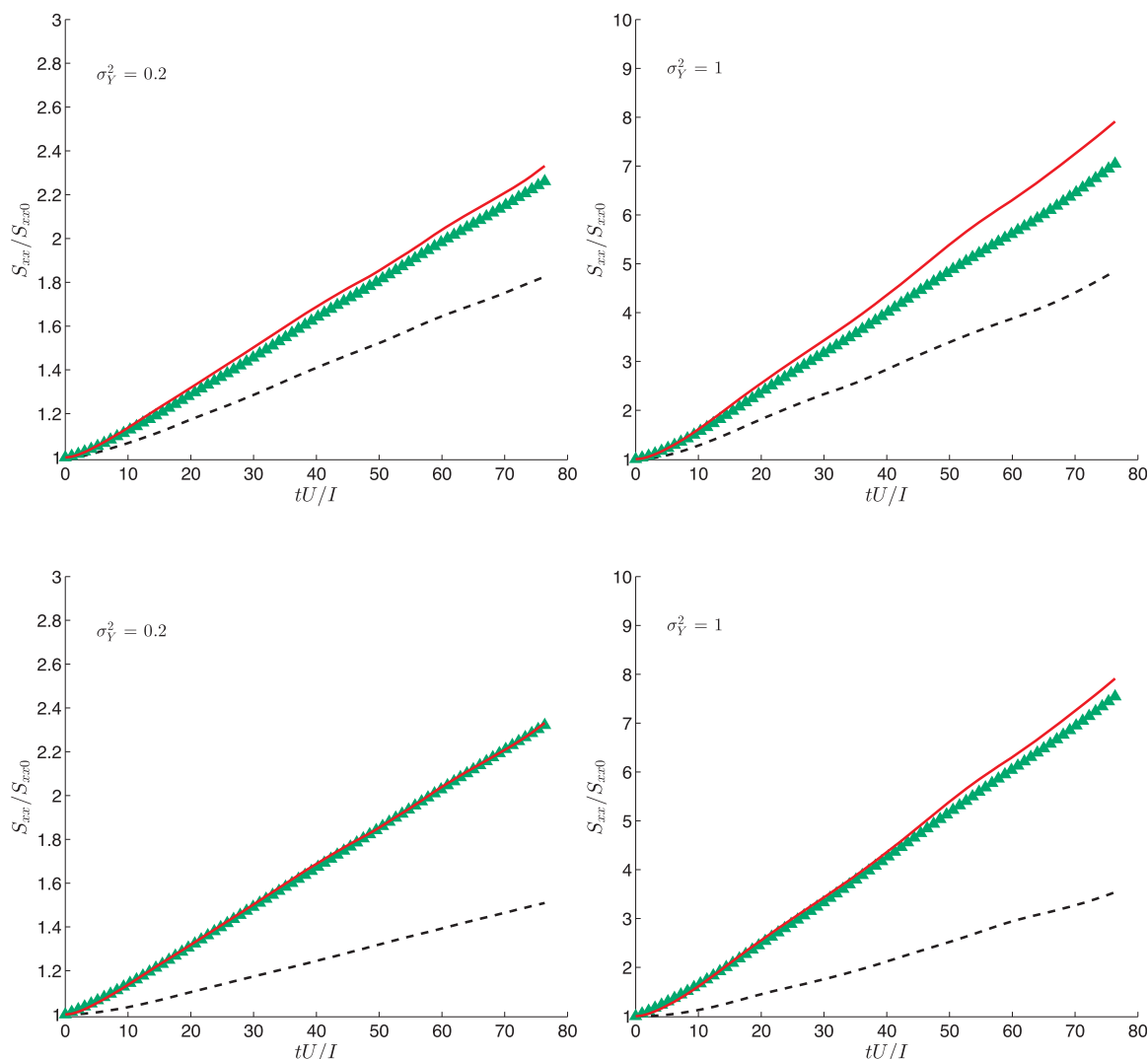


Figure 5. Second central spatial moment for fine (solid red), only coarse-grid velocity (dashed black) and coarse-grid velocity plus $D_b(\infty)$ (green triangles) for average of 10 realizations. Top row shows simulations for $\Delta_c = 16\Delta_f$ and bottom row for $\Delta_c = 32\Delta_f$.

average reaches an asymptotic value for even a smaller number of realizations. Figure 5 shows simulated S_{xx} versus time for $\sigma_Y^2=0.2, 1.0$ considering only fine-scale velocity, only coarse-scale velocity, and coarse-scale velocity and D_m^b evaluated at $t=\infty$. Simulations computed considering the coarse-grid-scale velocity show a significantly lower rate of spreading due to removing the high-frequency information of the velocity field from the coarse grid. For $\Delta_c=32\Delta$ the addition of D_m^b compensates for the missing information and the simulated rate of spreading is similar to the one observed for the fine-scale simulations. For the smaller coarse-block ($\Delta_c=16\Delta$) the addition of D_m^b also makes up for part of the lack of spreading, but there is still a noticeable difference with the fine-scale results at late times, particularly for $\sigma_Y^2=1$. We also run simulations for larger variances ($\sigma_Y^2=3, 6$, not shown here), but the results indicated that in those cases, as expected considering the first-order approximation used to derive it, D_m^b was not a good model for the lost subgrid-scale information. These results confirm the findings of previous studies [Rubin *et al.*, 1999, 2003; Bellin *et al.*, 2004] in the sense that the use of the block-scale macrodispersion coefficient in coarse-grid simulations is able to model the effect of the missing subgrid-scale information on spreading provided that the size of the coarse-grid cell is large in comparison to the heterogeneity length-scale (l_Y) and that σ_Y^2 is relatively small.

3.3.2. Mixing and Dilution

Preliminary simulations show that the variability for mixing among realizations is much less than for spreading, because mixing strongly depends upon local dispersion which is constant for all realizations. Based on this and considering that the simulations that include local-scale mass exchange through the SPH approximation are much more time-consuming than the ones that simulate only particle positions, we decided to only run three realizations for each scenario. To reproduce the mixing observed in fine-scale simulations, we simulate the stochastic component of the fluid particles movement using the block-scale effective dispersion coefficient D_e^b defined in Supporting Information and shown in Figure 4.

Figure 6 shows simulated concentrations after the initial plume has traveled $100\tau_u$ for different Pe values. By simple comparison of results computed on a fine grid with grid spacing Δ and a coarse grid with spacing $\Delta_c=16\Delta$, one can distinguish the lack of mixing of the coarse-grid simulations due to the lost subgrid-scale velocity. With the addition of a block-effective dispersion coefficient to simulate the missing spreading of the fluid particles due to the lost subgrid-scale velocity fluctuations, it is possible to compensate for the lack of mixing and reproduce the zone of low concentrations around the boundaries of the plume observed in the fine-scale simulations. However, the overall shape of the plume is much more regular than in the fine-scale simulations, which denotes a lack of spreading. Figure 7 shows a comparison between the reference solution computed with the velocity field calculated in the fine grid with results computed with the coarse-scale velocity ($\Delta_c=16\Delta$) field plus D_e^b . Simple inspection of this figure shows that even though small-scale spreading is lost in simulations that consider coarse-scale velocity fields, the area of the mixing zone that corresponds to intermediate values of concentrations is reasonably well reproduced.

The previous conclusions are confirmed by Figure 8 which shows the temporal evolution of the normalized scalar dissipation, SD (a figure with similar results for $\Delta_c=32\Delta$ is included in Supporting Information). These figures show that simulations using only the coarse-grid cell velocity underestimate mixing, which is indicated by the much lower slopes of the curves. The lack of mixing due to removing subgrid-scale velocity fluctuations is clear in all the simulated scenarios, even for high Pe values. On the other hand, the use of a constant block-scale macrodispersion coefficient evaluated at long-time ($D_m^b(\infty)$) overestimates, in most scenarios by a large margin, mixing rates observed in the fine-grid simulations. The use of a time-dependent block-scale effective dispersion coefficient leads to close reproduction of the dilution rates simulated in the fine grid during the simulated period.

It is interesting to note that the slopes of the fine and coarse-grid simulation with both dispersion coefficients, D_m^b and D_e^b , tend to be the same at the end of the simulated time for the cases with $Pe = 25$ and $Pe = 100$. This is expected since, as discussed in the previous sections, both coefficients become identical for times equal to or greater than the diffusive time scale τ_D , which for these scenarios is 25 and 100 advective time scales $\tau_u=U/l_Y$. Hence, this confirms that for low Péclet numbers it is possible to use a single dispersion coefficient that correctly represents spreading and mixing even at early time. However, for higher Péclet values mixing rates computed assuming a constant grid-scale dispersion coefficient are still very different from the results computed on the fine grid even after the plume has traveled more than 100 advective time scales. Moreover, following the previous reasoning to explain the results for low Pe , one can

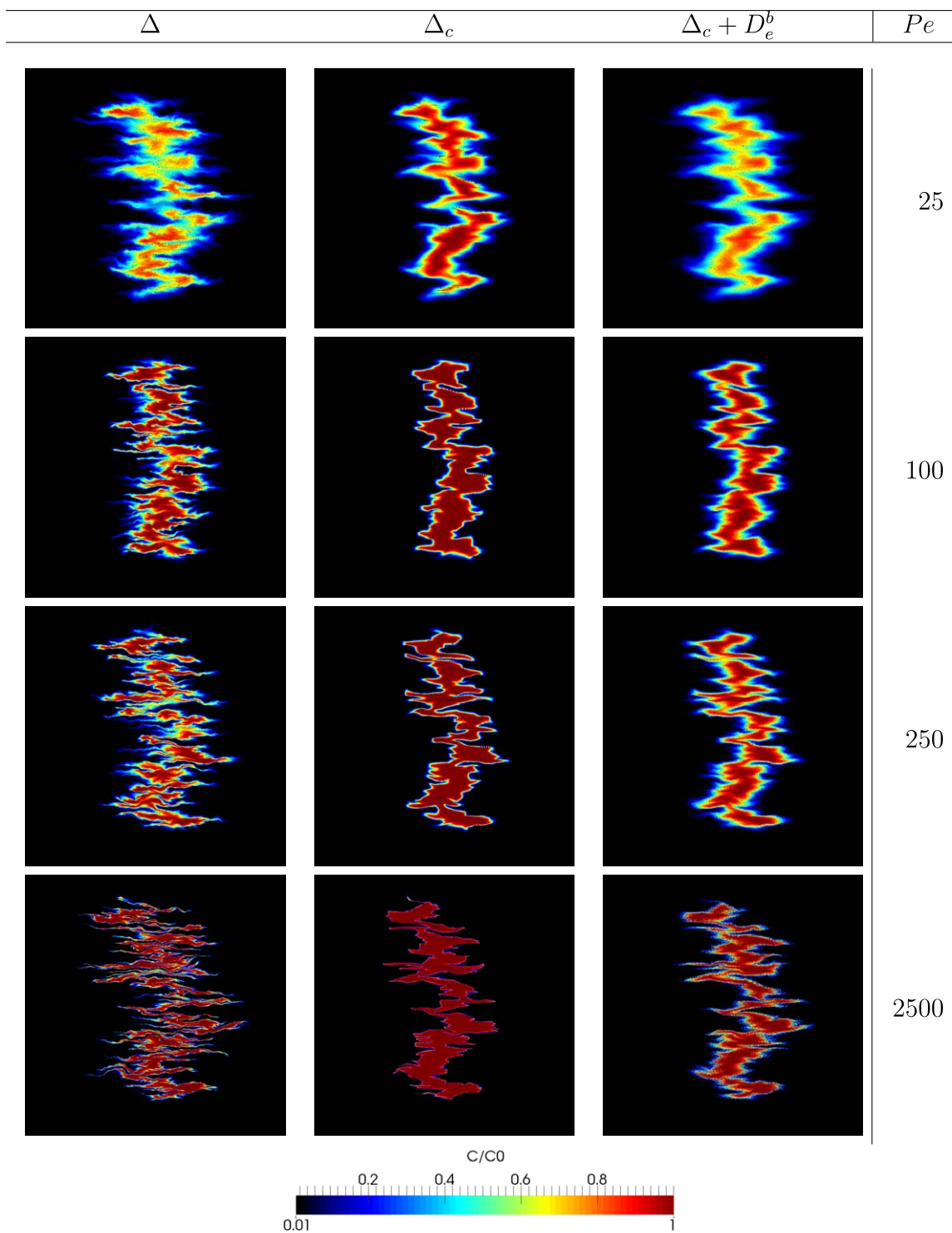


Figure 6. Simulated concentration distribution after the solute plume has traveled $100 \tau_d$. First, second, and third columns show simulated concentration with fine grid, only coarse-grid ($\Delta_c = 16\Delta$), and coarse-grid plus block-scale effective dispersion, respectively. The reduced size of the mixing zone (intermediate colors) for the figures in the second column indicates a lack of mixing with respect to the reference fine-scale simulation (first column).

expect that for advection-dominated situations, which are common in field applications, solute mixing and spreading can be represented by a single dispersion coefficient only after the plume has traveled thousands of advective time scales.

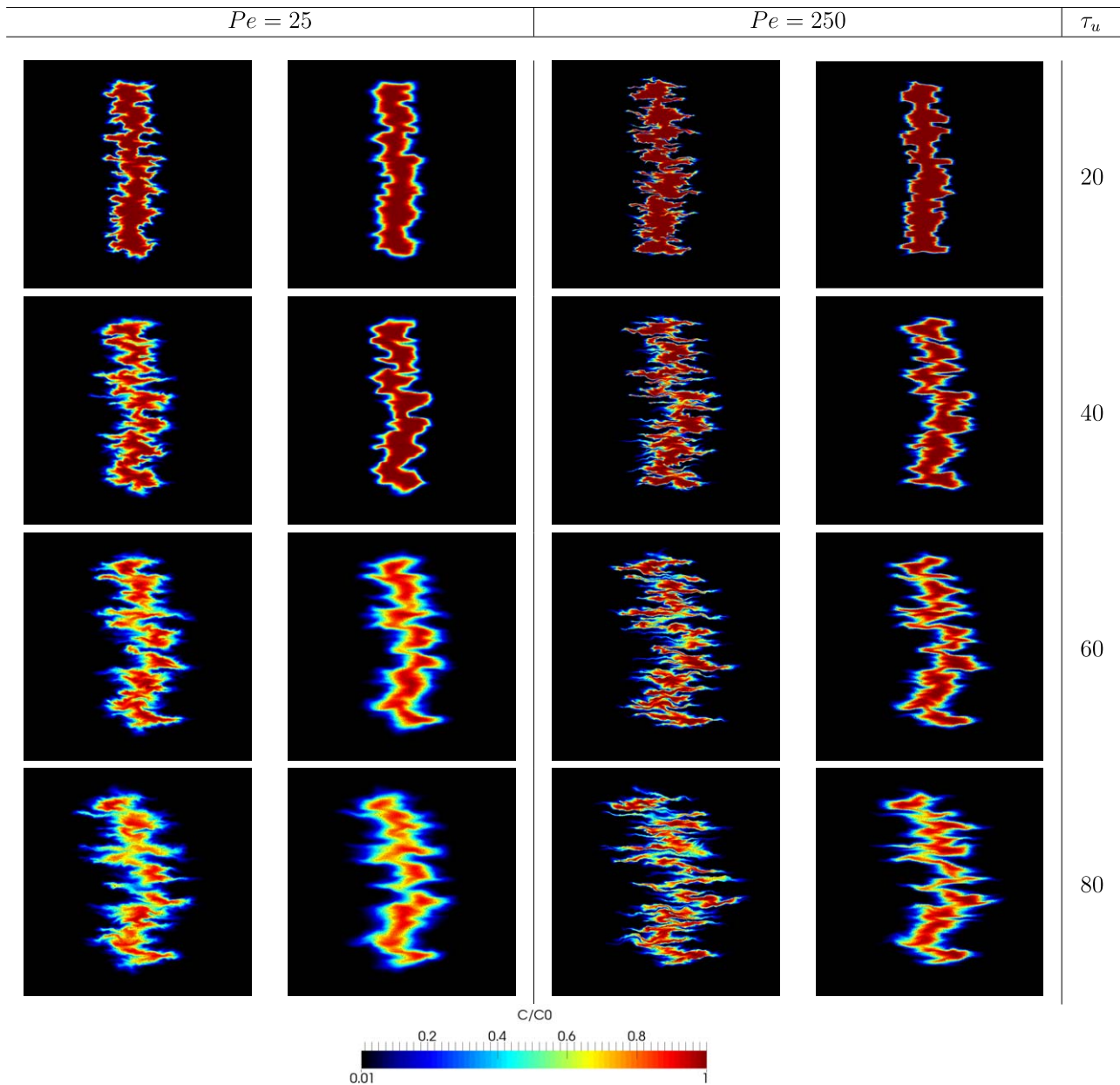


Figure 7. Simulated concentration distribution after the solute plume has traveled different advective time scales τ_u . First and third column show results computed with fine-grid velocity, while second and fourth columns show results computed considering coarse-grid velocity $\Delta_c = 16\Delta$ and effective block-scale dispersion coefficient.

The previous results are confirmed when observing the temporal behavior of the dilution index versus time shown in Figure 9 (a figure with similar results for $\Delta_c = 32\Delta$ is included in Supporting Information). The curves for coarse-grid simulations that include D_e^b are similar to the ones that correspond to the fine-scale simulations for all the scenarios simulated.

4. Conclusions

We applied a hybrid Lagrangian numerical approach to investigate the validity of using dispersion coefficients to account for subgrid-scale spreading and mixing in Darcy-scale numerical simulations of solute transport in mildly heterogeneous porous media. The novelty of the proposed approach is that it is naturally able to consider two different dispersion coefficients, one for advective spreading (macrodispersion) and

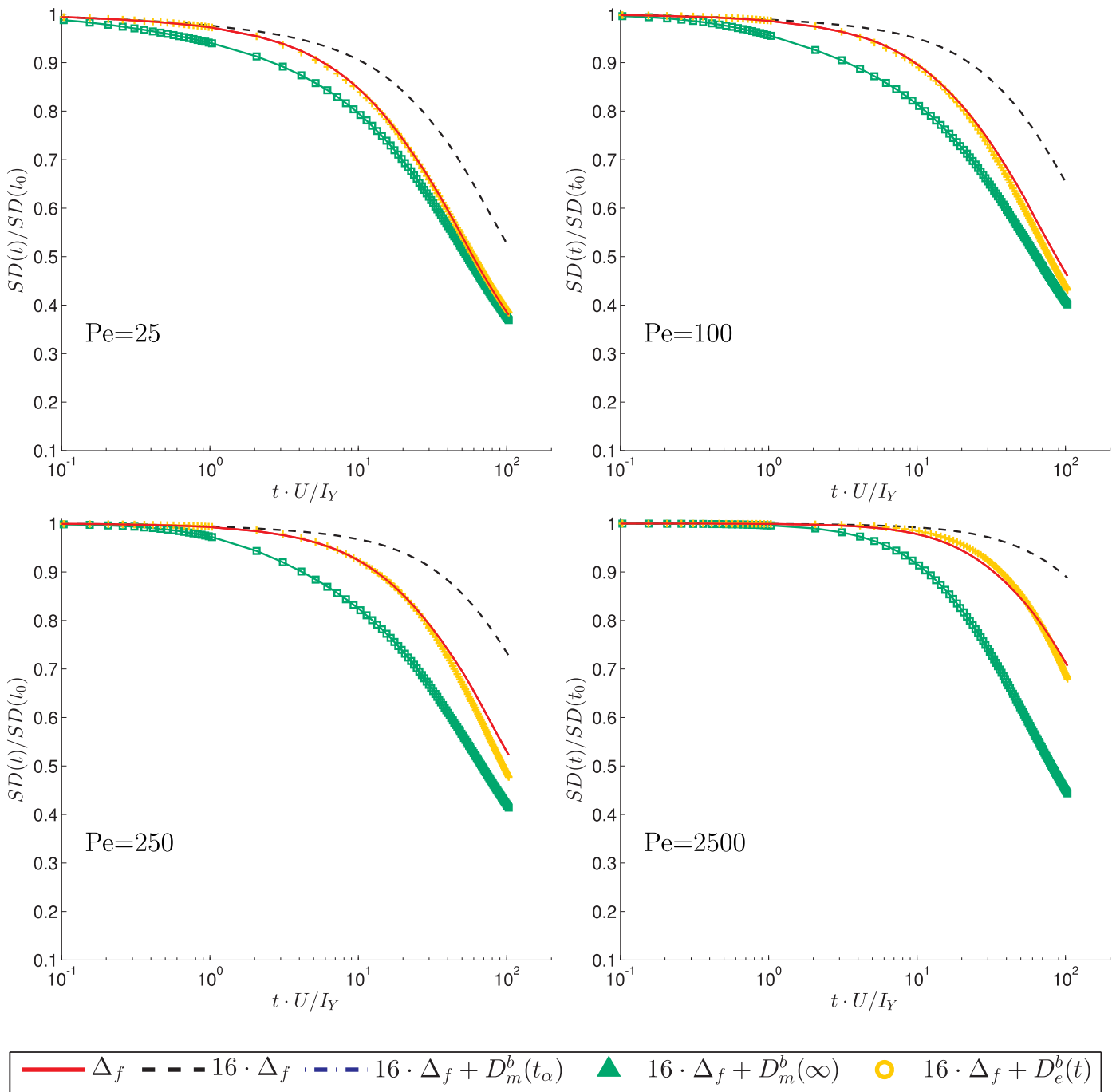


Figure 8. Normalized scalar dissipation (SD) computed as the ensemble mean of three realizations versus time for $\Delta_c = 16\Delta$.

the other for local dispersion. Moreover, the numerical scheme completely eliminates numerical dispersion, which usually adversely affects this type of study.

Through benchmark numerical simulations we demonstrated that:

1. It is possible to capture the effect of the lost subgrid-scale information on spreading and mixing by using block-scale dispersion coefficients to add a stochastic component to the movement of fluid particles. We use theoretical formulas for macro and effective dispersion developed by Rubin *et al.* [1999, 2003], Dentz *et al.* [2000a, 2000b], and Cirpka [2002]. This is convenient computationally, since it allows use of a small

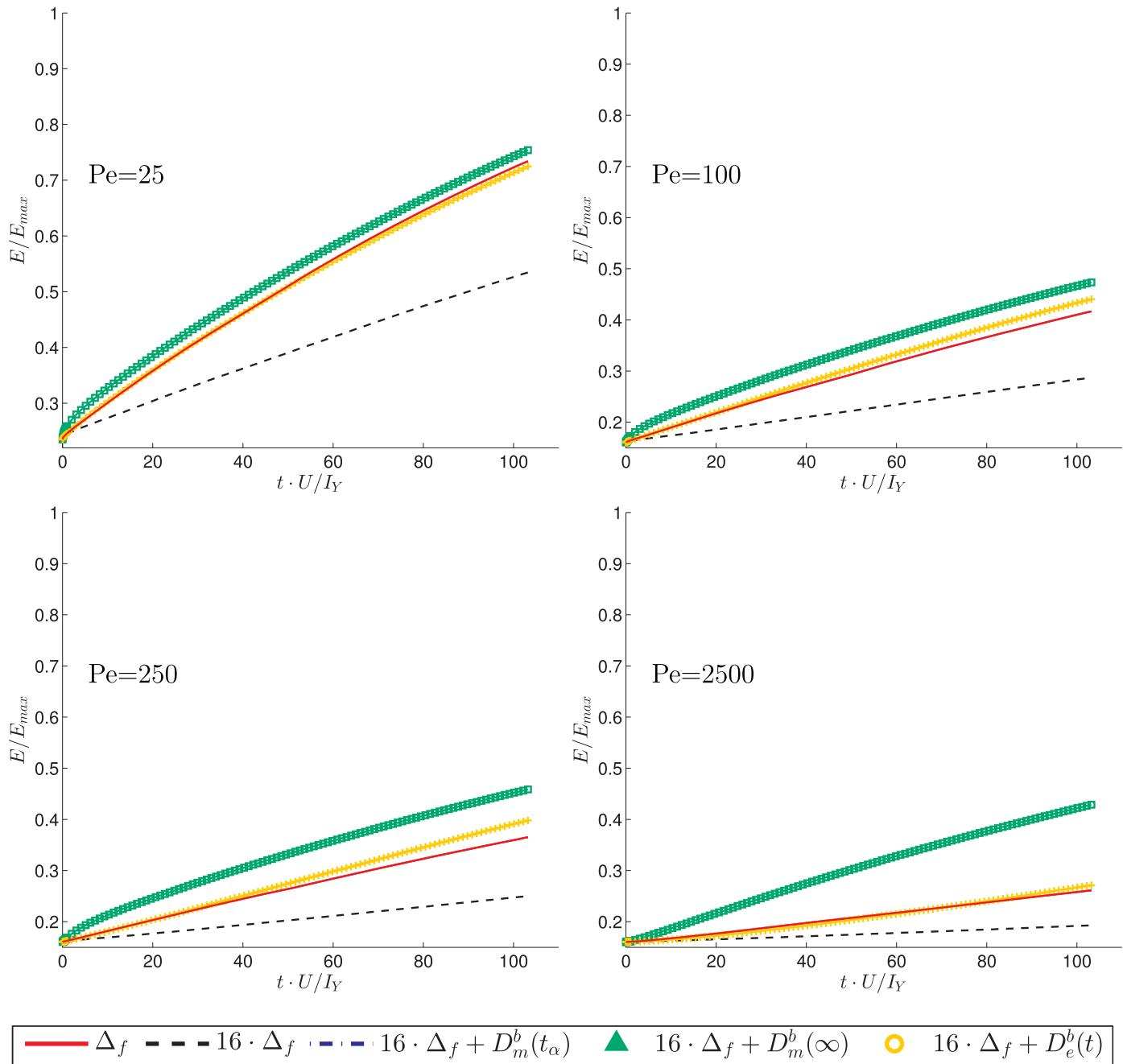


Figure 9. Normalized dilution index (E) computed as the ensemble mean of three realizations versus time for $\Delta_c = 16\Delta$.

number of realizations with large initial plumes. Our same overall numerical approach could be applied for the more realistic case of finite-sized plumes using the recent theory presented by *de Barros and Dentz* [2016].

2. To account only for spreading, it is possible to use a constant dispersion coefficient equal to asymptotic value of the block-scale macrodispersion coefficient, D_m^b , derived by *Rubin et al.* [1999].
3. To account only for mixing, it is necessary to use a time-dependent block-scale effective dispersion coefficient, D_e^b , which is equivalent to the effective dispersion coefficient proposed by *Dentz et al.* [2000a] and *Cirpka* [2002].
4. We verified that it is essential to consider that D_e^b depends upon the local-scale Péclet number and the grid size.

5. We found that for times larger than the typical diffusive time scale, τ_D , subgrid-scale spreading and mixing can be modeled by a single constant dispersion coefficient equal to the asymptotic limit of D_m^b .

Acknowledgments

The data for this manuscript can be requested by contacting the corresponding author. This work was funded by Conicyt Chile through project Fondecyt #11110228. A. J. Valocchi acknowledges financial support for a visit to Chile as part of this work. P. Herrera acknowledges financial support from the Fondap Project #15090013.

References

- Ababou, R., D. McLaughlin, L. W. Gelhar, and A. F. Tompson (1989), Numerical simulation of three-dimensional saturated flow in randomly heterogeneous porous media, *Transp. Porous Media*, 4(6), 549–565.
- Beckie, R. (1998), Analysis of scale effects in large-scale solute transport models, in *Scale Dependence and Scale Invariance in Hydrology*, pp. 314–334, Cambridge Univ. Press, Cambridge, U. K.
- Beckie, R., A. A. Aldama, and E. F. Wood (1994), The universal structure of the groundwater flow equations, *Water Resour. Res.*, 30(5), 1407–1419.
- Bellin, A., P. Salandin, and A. Rinaldo (1992), Simulation of dispersion in heterogeneous porous formations: Statistics, first-order theories, convergence of computations, *Water Resour. Res.*, 28(9), 2211–2227.
- Bellin, A., A. Lawrence, and Y. Rubin (2004), Models of sub-grid variability in numerical simulations of solute transport in heterogeneous porous formations: Three-dimensional flow and effect of pore-scale dispersion, *Stochastic Environ. Res. Risk Assess.*, 18(1), 31–38.
- Boso, F., A. Bellin, and M. Dumbser (2013), Numerical simulations of solute transport in highly heterogeneous formations: A comparison of alternative numerical schemes, *Adv. Water Resour.*, 52, 178–189.
- Chin, D. A. (1997), An assessment of first-order stochastic dispersion theories in porous media, *J. Hydrol.*, 199(1), 53–73.
- Chiogna, G., and A. Bellin (2013), Analytical solution for reactive solute transport considering incomplete mixing within a reference elementary volume, *Water Resour. Res.*, 49, 2589–2600, doi:10.1002/wrcr.20200.
- Chiogna, G., D. L. Hochstetler, A. Bellin, P. K. Kitanidis, and M. Rolle (2012), Mixing, entropy and reactive solute transport, *Geophys. Res. Lett.*, 39, L20405, doi:10.1029/2012GL053295.
- Cirpka, O. A. (2002), Choice of dispersion coefficients in reactive transport calculations on smoothed fields, *J. Contam. Hydrol.*, 58(3–4), 261–282, doi:10.1016/S0169-7722(02)00039-6.
- Cirpka, O. A., and W. Nowak (2003), Dispersion on kriged hydraulic conductivity fields, *Water Resources Research*, 39(2), 1027, doi:10.1029/2001WR000598.
- Dagan, G. (1984), Solute transport in heterogeneous porous formations, *J. Fluid Mech.*, 145, 151–177.
- Dagan, G. (1989), *Flow and Transport in Porous Formations*, Springer, Berlin.
- Dagan, G. (1990), Transport in heterogeneous porous formations: Spatial moments, ergodicity, and effective dispersion, *Water Resour. Res.*, 26(6), 1281–1290.
- Dagan, G. (1991), Dispersion of a passive solute in non-ergodic transport by steady velocity fields in heterogeneous formations, *J. Fluid Mech.*, 233, 197–210.
- Dai, Z., R. W. Ritz Jr., C. Huang, Y. N. Rubin, and D. F. Dominic (2004), Transport in heterogeneous sediments with multimodal conductivity and hierarchical organization across scales, *J. Hydrol.*, 294(1), 68–86.
- De Barros, F. P., and Y. Rubin (2011), Modelling of block-scale macrodispersion as a random function, *J. Fluid Mech.*, 676, 514–545.
- de Barros, F. P., and M. Dentz (2016), Pictures of blockscale transport: Effective versus ensemble dispersion and its uncertainty, *Adv. Water Resour.*, 91, 11–22.
- de Dreuzy, J.-R., J. Carrera, M. Dentz, and T. Le Borgne (2012), Time evolution of mixing in heterogeneous porous media, *Water Resour. Res.*, 48, W06511, doi:10.1029/2011WR011360.
- De Marsily, G., F. Delay, J. Gonçalves, P. Renard, V. Teles, and S. Violette (2005), Dealing with spatial heterogeneity, *Hydrogeol. J.*, 13(1), 161–183.
- Dentz, M., H. Kinzelbach, S. Attinger, and W. Kinzelbach (2000a), Temporal behavior of a solute cloud in a heterogeneous porous medium: 1. Point-like injection, *Water Resour. Res.*, 36(12), 3591–3604.
- Dentz, M., H. Kinzelbach, S. Attinger, and W. Kinzelbach (2000b), Temporal behavior of a solute cloud in a heterogeneous porous medium: 2. Spatially extended injection, *Water Resour. Res.*, 36(12), 3605–3614.
- Dentz, M., T. Le Borgne, A. Engler, and B. Bijeljic (2011), Mixing, spreading and reaction in heterogeneous media: A brief review, *J. Contam. Hydrol.*, 120, 1–17.
- Dogan, M., R. Van Dam, G. Liu, M. Meerschaert, J. Butler, G. Bohling, D. Benson, and D. Hyndman (2014), Predicting flow and transport in highly heterogeneous alluvial aquifers, *Geophys. Res. Lett.*, 41(21), 7560–7565.
- Eberhard, J. (2005), Upscaling for stationary transport in heterogeneous porous media, *Multiscale Model. Simul.*, 3(4), 957–976.
- Efendiev, Y., and L. Durlafsky (2003), A generalized convection-diffusion model for subgrid transport in porous media, *Multiscale Model. Simul.*, 1(3), 504–526.
- Fernández-García, D., and J. J. Gómez-Hernández (2007), Impact of upscaling on solute transport: Traveltimes, scale dependence of dispersivity, and propagation of uncertainty, *Water Resour. Res.*, 43, W02423, doi:10.1029/2005WR004727.
- Fernández-García, D., and X. Sanchez-Vila (2011), Optimal reconstruction of concentrations, gradients and reaction rates from particle distributions, *J. Contam. Hydrol.*, 120, 99–114.
- Fiori, A. (1996), Finite Peclet extensions of Dagan's solutions to transport in anisotropic heterogeneous formations, *Water Resour. Res.*, 32(1), 193–198.
- Gelhar, L. W. (1993), *Stochastic Subsurface Hydrology*, Prentice Hall, Englewood Cliffs.
- Gelhar, L. W., and C. L. Axness (1983), Three-dimensional stochastic analysis of macrodispersion in aquifers, *Water Resour. Res.*, 19(1), 161–180.
- Herrera, P. A., and R. D. Beckie (2013), An assessment of particle methods for approximating anisotropic dispersion, *Int. J. Numer. Methods Fluids*, 71(5), 634–651.
- Herrera, P. A., M. Massabó, and R. D. Beckie (2009), A meshless method to simulate solute transport in heterogeneous porous media, *Adv. Water Resour.*, 32(3), 413–429.
- Herrera, P. A., A. J. Valocchi, and R. D. Beckie (2010), A multidimensional streamline-based method to simulate reactive solute transport in heterogeneous porous media, *Adv. Water Resour.*, 33(7), 711–727.
- Hinnell, A., T. Ferré, J. Vrugt, J. Huisman, S. Moysey, J. Rings, and M. Kowalsky (2010), Improved extraction of hydrologic information from geophysical data through coupled hydrogeophysical inversion, *Water Resour. Res.*, 46, W00D40, doi:10.1029/2008WR007060.
- Jadoon, K. Z., E. Slob, M. Vanclooster, H. Vereecken, and S. Lambot (2008), Uniqueness and stability analysis of hydrogeophysical inversion for time-lapse ground-penetrating radar estimates of shallow soil hydraulic properties, *Water Resour. Res.*, 44, W09421, doi:10.1029/2007WR006639.

- Janssen, G. M., O. A. Cirpka, and S. E. Van der Zee (2006), Stochastic analysis of nonlinear biodegradation in regimes controlled by both chromatographic and dispersive mixing, *Water Resour. Res.*, *42*, W01417, doi:10.1029/2005WR004042.
- Kapoor, V., and P. K. Kitanidis (1997), Advection-diffusion in spatially random flows: Formulation of concentration covariance, *Stochastic Hydrol. Hydraul.*, *11*(5), 397–422.
- Kapoor, V., and P. K. Kitanidis (1998), Concentration fluctuations and dilution in aquifers, *Water Resour. Res.*, *34*(5), 1181–1193.
- Kitanidis, P. K. (1988), Prediction by the method of moments of transport in a heterogeneous formation, *J. Hydrolo.*, *102*(1), 453–473.
- Kitanidis, P. K. (1994), The concept of the dilution index, *Water Resour. Res.*, *30*(7), 2011–2026.
- Lambot, S., A. Binley, E. Slob, and S. Hubbard (2008), Ground penetrating radar in hydrogeophysics, *Vadose Zone J.*, *7*(1), 137–139.
- Le Borgne, T., M. Dentz, D. Bolster, J. Carrera, J.-R. De Dreuzy, and P. Davy (2010), Non-Fickian mixing: Temporal evolution of the scalar dissipation rate in heterogeneous porous media, *Adv. Water Resour.*, *33*(12), 1468–1475.
- Lichtner, P. C., S. Kelkar, and B. Robinson (2002), New form of dispersion tensor for axisymmetric porous media with implementation in particle tracking, *Water Resour. Res.*, *38*(8), 1146, doi:10.1029/2000WR001100.
- Pope, S. B. (2000), *Turbulent Flows*, Cambridge Univ. Press, Cambridge, U. K.
- Quinodoz, H. A., and A. J. Valocchi (1993), Stochastic analysis of the transport of kinetically sorbing solutes in aquifers with randomly heterogeneous hydraulic conductivity, *Water Resour. Res.*, *29*(9), 3227–3240.
- Rajaram, H., and L. W. Gelhar (1993), Plume scale-dependent dispersion in heterogeneous aquifers: 1. Lagrangian analysis in a stratified aquifer, *Water Resour. Res.*, *29*(9), 3249–3260.
- Renard, P., and G. de Marsily (1997), Calculating equivalent permeability: A review, *Adv. Water Resour.*, *20*(5), 253–278.
- Ritzi, R., D. Jayne, A. Zahradiq, A. Field, and G. Fogg (1994), Geostatistical modeling of heterogeneity in glaciofluvial, buried-valley aquifers, *Ground Water*, *32*(4), 666–674.
- Robin, M., A. Gutjahr, E. Sudicky, and J. Wilson (1993), Cross-correlated random field generation with the direct Fourier transform method, *Water Resour. Res.*, *29*(7), 2385–2397.
- Rolle, M., C. Eberhardt, G. Chiogna, O. A. Cirpka, and P. Grathwohl (2009), Enhancement of dilution and transverse reactive mixing in porous media: Experiments and model-based interpretation, *J. Contam. Hydrol.*, *110*(3), 130–142.
- Rubin, Y. (2003), *Applied Stochastic Hydrogeology*, Oxford Univ. Press, Oxford, U. K.
- Rubin, Y., A. Sun, R. Maxwell, and A. Bellin (1999), The concept of block-effective macrodispersivity and a unified approach for grid-scale and plume-scale-dependent transport, *J. Fluid Mech.*, *395*, 161–180.
- Rubin, Y., A. Bellin, and A. E. Lawrence (2003), On the use of block-effective macrodispersion for numerical simulations of transport in heterogeneous formations, *Water Resour. Res.*, *39*(9), 1242, doi:10.1029/2002WR001727.
- Salamon, P., D. Fernández-García, and J. J. Gómez-Hernández (2006), A review and numerical assessment of the random walk particle tracking method, *J. Contam. Hydrol.*, *87*(3), 277–305.
- Salandin, P., and V. Fiorotto (1998), Solute transport in highly heterogeneous aquifers, *Water Resour. Res.*, *34*(5), 949–961.
- Scheibe, T., and D. Freyberg (1990), Impacts of geological structure on transport: Creating a data base, in *Fifth Canadian/American Conference on Hydrogeology*, edited by S. Bachu, pp. 56–71, Alberta Research Council, Calgary, Alberta.
- Tartakovsky, A., N. Trask, K. Pan, B. Jones, W. Pan, and J. Williams (2015), Smoothed particle hydrodynamics and its applications for multi-phase flow and reactive transport in porous media, *Comput. Geosci.*, *20*, 807–834.
- Tartakovsky, A. M. (2010), Langevin model for reactive transport in porous media, *Phys. Rev. E*, *82*(2), 026302.
- Tartakovsky, A. M., D. M. Tartakovsky, and P. Meakin (2008), Stochastic Langevin model for flow and transport in porous media, *Phys. Rev. Lett.*, *101*(4), 044502.
- Trefry, M., F. Ruan, and D. McLaughlin (2003), Numerical simulations of preasymptotic transport in heterogeneous porous media: Departures from the Gaussian limit, *Water Resour. Res.*, *39*(3), 1063, doi:10.1029/2001WR001101.
- Urroz, G. E., Y. Ma, and M. W. Kemblowski (1995), Advective and dispersive mixing in stratified formations, *Transp. Porous Media*, *18*(3), 231–243.
- Ursino, N., T. Gimmi, and H. Flüher (2001), Dilution of non-reactive tracers in variably saturated sandy structures, *Adv. Water Resour.*, *24*(8), 877–885.
- Wainwright, H. M., J. Chen, D. S. Sassen, and S. S. Hubbard (2014), Bayesian hierarchical approach and geophysical data sets for estimation of reactive facies over plume scales, *Water Resour. Res.*, *50*, 4564–4584, doi:10.1002/2013WR013842.
- Weeks, S. W., and G. Sposito (1998), Mixing and stretching efficiency in steady and unsteady groundwater flows, *Water Resour. Res.*, *34*(12), 3315–3322.
- Wu, J., B. X. Hu, and D. Zhang (2003), Applications of nonstationary stochastic theory to solute transport in multi-scale geological media, *J. Hydrol.*, *275*(3), 208–228.
- Zhang, D., R. Andricevic, A. Y. Sun, X. Hu, and G. He (2000), Solute flux approach to transport through spatially nonstationary flow in porous media, *Water Resour. Res.*, *36*(8), 2107–2120.
- Zheng, C., M. Bianchi, and S. M. Gorelick (2011), Lessons learned from 25 years of research at the made site, *Ground Water*, *49*(5), 649–662.